ISSN 1674-1056
http://cpb.iphy.ac.cn
http://iopscience.iop.org/cpb
中国物理 B
Chinese Physics
中国物理 Chinese Physics B

Structural stability and vibrational characteristics of CaB_6 under high pressure

Mingkun Liu(刘明坤), Can Tian(田灿), Xiaoli Huang(黄晓丽), Fangfei Li(李芳菲), Yanping Huang(黄艳萍), Bingbing Liu(刘冰冰), Tian Cui(崔田)

Citation: Chin. Phys. B . 2019, 28(6): 068101. **doi:** 10.1088/1674-1056/28/6/068101
Journal homepage: http://cpb.iphy.ac.cn; http://iopscience.iop.org/cpb

What follows is a list of articles you may be interested in

Inclusions in large diamond single crystals at different temperatures of synthesis

Fei Han(韩飞), Shang-Sheng Li(李尚升), Xue-Fei Jia(贾雪菲), Wei-Qin Chen(陈玮琴), Tai-Chao Su(宿太超), Mei-Hua Hu(胡美华), Kun-Peng Yu(于昆鹏), Jian-Kang Wang(王健康), Yu-Min Wu(吴玉敏), Hong-An Ma(马红安), Xiao-Peng Jia(贾晓鹏)

Chin. Phys. B . 2019, 28(2): 028103. **doi:** 10.1088/1674-1056/28/2/028103

Synthesis of diamonds in Fe—C systems using nitrogen and hydrogen co-doped impurities under HPHT

Shi-Shuai Sun(孙士帅), Zhi-Hui Xu(徐智慧), Wen Cui(崔雯), Xiao-Peng Jia(贾晓鹏), Hong-An Ma(马红安)

Chin. Phys. B . 2017, 26(9): 098101. **doi:** 10.1088/1674-1056/26/9/098101

Different effect of NiMnCo or FeNiCo on the growth of type-IIa large diamonds with Ti/Cu as nitrogen getter

Shang-Sheng Li(李尚升), He Zhang(张贺), Tai-Chao Su(宿太超), Qiang Hu(胡强), Mei-Hua Hu(胡美华), Chun-Sheng Gong(龚春生), Hon-An Ma(马红安), Xiao-Peng Jia(贾晓鹏), Yong Li(李勇)

Chin. Phys. B . 2017, 26(6): 068102. **doi:** 10.1088/1674-1056/26/6/068102

Synthesis of N-type semiconductor diamonds with sulfur, boron co-doping in FeNiMnCo-C system at high pressure and high temperature

He Zhang(张贺), Shangsheng Li(李尚升), Taichao Su(宿太超), Meihua Hu(胡美华), Hongan Ma(马红安), Xiaopeng Jia(贾晓鹏), Yong Li(李勇)

Chin. Phys. B . 2017, 26(5): 058102. **doi:** 10.1088/1674-1056/26/5/058102

High thermal stability of diamond-cBN-B_4C-Si composites

Hong-Sheng Jia(贾洪声), Pin-Wen Zhu(朱品文), Hao Ye(叶灏), Bin Zuo(左斌), Yuan-Long E(鄂元龙), Shi-Chong Xu(徐仕翀), Ji Li(李季), Hai-Bo Li(李海波), Xiao-Peng Jia(贾晓鹏), Hong-An Ma(马红安)

Chin. Phys. B . 2017, 26(1): 018102. **doi:** 10.1088/1674-1056/26/1/018102

Structural stability and vibrational characteristics of CaB_6 under high pressure*

Mingkun Liu(刘明坤), Can Tian(田灿), Xiaoli Huang(黄晓丽)†, Fangfei Li(李芳菲), Yanping Huang(黄艳萍), Bingbing Liu(刘冰冰), and Tian Cui(崔田)

State Key Laboratory of Superhard Materials, College of Physics, Jilin University, Changchun 130012, *China*

(Received 7 January 2019; revised manuscript received 4 April 2019; published online 8 May 2019)

In situ Raman spectroscopy and x-ray diffraction measurements are used to explore the structural stability of CaB_6 at high pressures and room temperature. The results show no evidence of structural phase transitions up to at least 40 GPa. The obtained equation of state with smooth pressure dependencies yields a zero-pressure isothermal bulk modulus $B_0 =$ 170 (5) GPa, which agrees well with the previous measurements. The frequency shifts for A_{1g}, E_g, and T_{2g} vibrational modes of polycrystalline CaB_6 are obtained with pressure uploading. As the pressure increases, all the vibration modes have smooth monotonic pressure dependence. The Grüneisen parameter of E_g modes is the largest, indicating its largest dependence on the volume of a crystal lattice.

Keywords: CaB_6, high pressure, diamond anvil cell, structural stability

PACS: 81.05.Je, 81.05.ug, 91.65.Pj, 64.60.–i **DOI:** 10.1088/1674-1056/28/6/068101

1. Introduction

The hexaborides MB_6 of the rare earth elements and the alkaline earth elements, such as YB_6, CeB_6, SrB_6, and BaB_6, have long been popular topics of theoretical and experimental studies.[1–4] These hexaborides crystallize in a CsCl-type structure with the alkaline earth element or rare earth atom and the octahedral B_6 molecules. Among these hexaborides, the trivalent rare earth hexaborides show novel physical properties, such as YB_6 with superconductivity, CeB_6 with dense Kondo behavior, and SmB_6 with intermediate valence state.[5–7] The divalent alkaline-earth hexaborides are renowned for having properties of high melting point and hardness, low density and coefficient of thermal expansion, and excellent chemical stability.[8–11]

At present, semiconductor CaB_6 with high Curie temperature has received much attention.[12–14] CaB_6 doped with small quantities of La contains no magnetic ions with an electron density of 7×10^{19} cm^{-3}. At the magnetic ordering temperature about 600 K, its ground state is ferromagnetically polarized with a saturation moment of 0.07 μ_b per electron. Considerable experimental and theoretical work is carried out for CaB_6 towards understanding this unexpected phenomenon. The theoretical calculations have given some explanations including ferromagnetic phase of the conventional itinerant magnetism, dilute electron gas, and the doped excitonic insulator.[15] Furthermore, Cho *et al.* have studied CaB_6 with 99.9999% (6N) purity boron and 99.9% (3N) purity boron by electrical measurements, and reported that CaB_6 with higher purity boron exhibited semiconducting features and another one exhibited metal properties.[16] Therefore, it can be concluded that the dramatic change in the electrical properties of CaB_6 is affected by the boron purity and the preparing conditions.

Pressure is an efficient method for changing the structures and properties of materials. Metal hexaborides such as LaB_6 and EuB_6 have been the focus in high-pressure study.[17,18] The LaB_6 structure was indexed as Pban but was not observed in subsequent experiments. Several studies on CaB_6 under extreme conditions have recently been reported. The earliest high pressure study of CaB_6 was fulfilled by *in situ* resistance measurement and energy dispersive x-ray diffraction (XRD) with the sample loaded in the diamond anvil cell (DAC).[19] Two phase transitions under high pressure were discovered: an electronic transition occurs at 3.7 GPa, and a structural phase transition occurs at 12 GPa with the CsCl-type structure transformed to orthogonal structure. Subsequently, an unexpectedly complex crystal structure of CaB_6 (space group: $I4/mmm$) was reported under high pressure and temperatures.[20] In theory, density functional theory (DFT) calculations predicted several structural transitions based on the dynamically stability.[21] However, the inconsistency between theory and experiment still exists, which needs further studies.

In this work, we report a joint of synchrotron XRD and Raman spectra study of CaB_6 up to 40 GPa to explore its crystal structures and vibrational properties. Synchrotron XRD and Raman spectroscopy have proven to be powerful tools to

*Project supported by the National Natural Science Foundation of China (Grant Nos. 51572108, 51632002, 11504127, 11674122, 11574112, 11474127, and 11634004), the 111 Project, China (Grant No. B12011), the Program for Changjiang Scholars and Innovative Research Team in University, China (Grant No. IRT_15R23), and the National Found for Fostering Talents of Basic Science, China (Grant No. J1103202).

†Corresponding author. E-mail: huangxiaoli@jlu.edu.cn

© 2019 Chinese Physical Society and IOP Publishing Ltd

investigate the structural properties under high pressure. The present work will also provide new insights into the structural stability of other metal hexaborides.

2. Experimental and theoretical methods

The powder sample was purchased from the Alfa Aesar Products, and loaded in the DAC with 400 μm. The sample chamber was made on a T-301 stainless steel gasket by laser beam drilling machine. Its diameter was 120 μm and the thick was 55 μm. The methanol–ethanol mixture with a volume ratio of 4:1 was used for pressure-transmitting media.[22] The pressure was determined by ruby fluorescence R1 peaks inside the sample chamber.[23]

The Raman spectra were measured by an ActonSpetraPro500i spectrograph with a liquid-nitrogen-cooled charge-coupled device (CCD) detector. The excitation laser wavelength was 532 nm and laser power was 10 mW. The acquisition time for each experiment was 200 s, and the experimental data was analysed by OriginPro 8.5 software.

In situ high-pressure angle-dispersive XRD experiments were carried out at the 16-BM-D station of High Pressure Collaborative Access Team (HPCAT), Advanced Photon Source, Argonne National Laboratory. A focused monochromatic x-ray beam was used for measurement. Its diameter was 13 μm and the wavelength was 0.4122 Å. The acquisition time was adjusted as 300 s in order to get clear XRD data. The geometric parameters were calibrated by CeO_2 standard. The image plate area detector (Mar345) was used to record the Bragg diffraction rings, and Fit2D software was used to convert the Bragg diffraction rings into plots of intensity.[24] The XRD patterns were fitted by Rietveld profile matching of the Materials Studio program.[25]

3. Results and discussions

As one of the divalent alkaline-earth hexaborides, CaB_6 crystallizes into a CsCl-type structure with the space group of *Pm*-3*m* under ambient pressure.[26] There is one molecule in the unit cell. The crystal structure of CaB_6 under ambient conditions is shown in the inset of Fig. 1. A boron octahedral cage is located at the cubic center and metal ions (Ca) are located at the cubic corners. In Fig. 1, the refinement of CaB_6 carried out on an XRD pattern is shown at about 1.9 GPa. The refined lattice constant a is 4.148 (2) Å, and unit cell volume V is 71.35 (9) Å^3 which matches well with previous report.[27]

Synchrotron XRD experiments are carried out to trigger the structural changes of CaB_6 under high pressure. The representative XRD patterns of CaB_6 with pressure uploading are shown in Fig. 2. The pressure is compressed up to 35 GPa in this experiment. As pressure increases, all diffraction peaks shift to higher 2θ angles, showing the crystalline interplanar spacing decreases gradually. In addition, the Bragg peaks are broadened. However, no new peaks are observed up to 35.2 GPa, indicating that no phase transition occurs with pressure uploading. So the cubic structure of CaB_6 appears to be quite stable with pressure up to 35 GPa. Meanwhile, as pressure decreases to ambient pressure, the cubic structure of CaB_6 is obtained. As for the work of Li Ming *et al.*, an electronic transition occurs at 3.7 GPa, and a structural phase transition occurs at 12 GPa, with the CsCl-type structure transformed to orthogonal structure.[19] And the study of Kolmogorov *et al.* showed that *Cmcm* is the lowest enthalpy structure for 13 GP-32 GPa pressures, and $I4/mmm$ is a new ground state candidate above 32 GPa.[20] A different result has been obtained in our experiment—up to 35.2 GPa, no new peaks are observed, which means that the structure of CaB_6 remains stable up to 35 GPa. All the XRD patterns are refined by Rietveld full profile structure. The refined lattice constants and volume of CaB_6 as a function of pressure are shown in Fig. 3, which are obtained by Rietveld refinements using Materials Studio software. All the relative unit-cell volumes with pressure changes are fitted to a third-order Birch-Murnaghan equation of state (EOS)[28]

$$P = \frac{3B_0}{2}\left[\left(\frac{V}{V_0}\right)^{-7/3} - \left(\frac{V}{V_0}\right)^{-5/3}\right] \times \left\{1 + \frac{3}{4}\left(B_0' - 4\right)\left[\left(\frac{V}{V_0}\right)^{-2/3} - 1\right]\right\}.$$

In the formula, B represents the isothermal bulk modulus, B' represents the first derivative of the bulk modulus versus pressure, V represents the volume per formula unit under ambient pressure, and V represents the volume per formula unit at given pressure P. The lattice parameter monotonically decreases with pressure uploading, which indicates the preservation of the original structure. We have used $V = 71.6$ Å^3 from experiments to constrain the equation of state.[29] By fitting, as shown in Fig. 3, results are obtained as $B_0 = 170$ (5) GPa with B' fixed at 4.

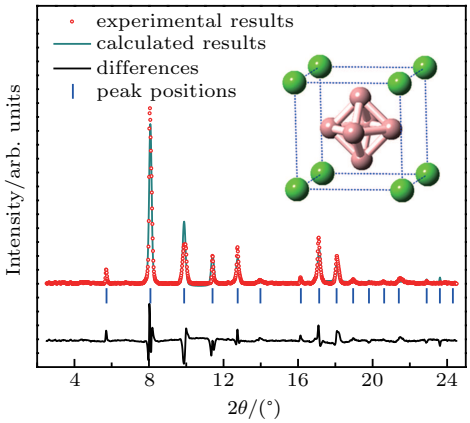


Fig. 1. Full profile Rietveld structural refinement of CaB_6 under high pressure. The fit has an R_{wp} of 2.0% and the calculated intensities are in good agreement with the observed intensities. The pattern is collected at 1.9 GPa with the incident x-ray wavelength of 0.4122 Å. The crystal structure of CaB_6 is shown in the illustration.

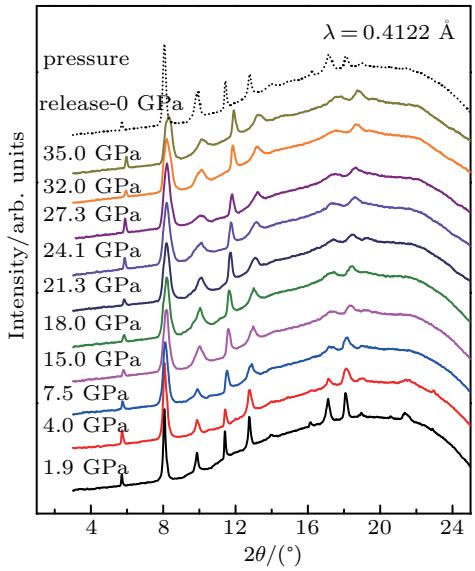


Fig. 2. Selected angle dispersive x-ray diffraction patterns of CaB_6 with pressure range from 1.9 GPa to 35.0 GPa. The top dotted line represents the pattern upon decompression to ambient pressure.

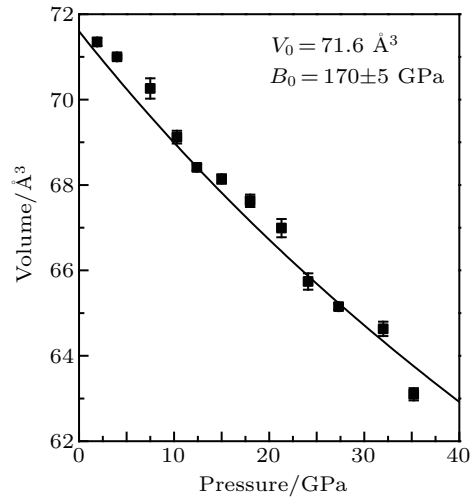


Fig. 3. The volume of CaB_6 at different pressures. The square symbols represent experiment data, and solid-black lines are the results after fitting. The pressure-volume data is fitted by third-order Birch–Murnaghan equation of state.

Table 1. The volume and corresponding errors of CaB_6 at different pressures.

Pressure/GPa	Volume/Å^3	Errors/Å^3
1.9	71.35	0.09
4.	71.00	0.03
7.5	70.26	0.24
10.3	69.12	0.15
12.4	68.41	0.08
15.	68.14	0.11
18.	67.63	0.15
21.3	66.99	0.21
24.1	65.74	0.19
27.3	65.15	0.07
32.	64.63	0.17
35.2	63.1	0.14

Raman spectroscopy has proven to be useful to study the vibrational properties and structural changes under high pressure.[30–32] We also have performed high-pressure Raman spectra to confirm the results from XRD patterns. The representation for the optical vibration modes of $q = 0$ (center of Brillouin zone) with point group O_h for CaB_6 was predicted with group theory as follows:[33]

$$\Gamma = A_{1g}^{R} + E_{g}^{R} + T_{1g} + T_{2g}^{R} + 3T_{1u} + T_{2u},$$

where A_{1g}, E_g, and T_{2g} represent Raman-active modes, one of three T_{1u} modes is acoustic mode, the other two represent infrared-active mode, and T_{1g} and T_{2u} are optically inactive.

Figure 4 shows the measured Raman spectra of CaB_6 under ambient pressure. This shows that there are four peaks centered at 777 cm^{-1}, 1137 cm^{-1}, 1147 cm^{-1}, and 1279 cm^{-1}, and the results are in agreement with previous report.[16] These vibration modes are related with the boron octahedron. For the three vibration modes, T_{2g} is triply degenerate symmetric bending vibration mode, E_g is double degenerate symmetric stretch vibration mode, and A_{1g} is nondegenerate symmetric stretch vibration mode. Besides, it is known that E_g mode is a broad single peak for the trivalent hexaborides case but a doublet for divalent.[33] Figures 4(b)–4(d) specifically show T_{2g}, E_g, and A_{1g} vibration modes, respectively.

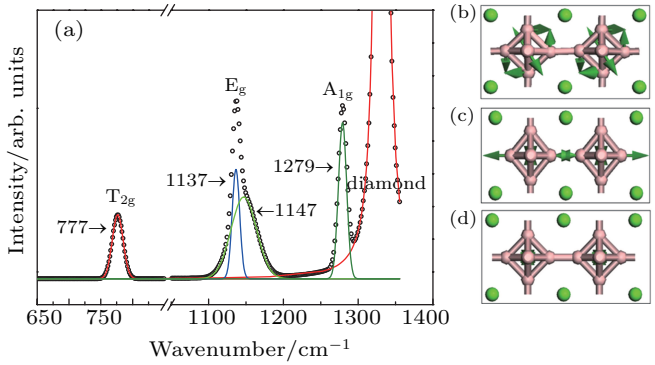


Fig. 4. (a) The Raman spectra of CaB_6 measured under ambient pressure, and panels (b), (c), and (d) represent T_{2g}, E_g, and A_{1g} vibration modes, respectively.

High-pressure Raman spectra are measured up to 40 GPa. The selected Raman spectra with pressure increasing are shown in Fig. 5(a). The corresponding Raman frequency shifts with pressure are shown in Fig. 5(b). In the whole pressure range, in Fig. 5(a), it is noticed that the wavenumber of the T_{2g} and A_{1g} vibration modes blueshifts with pressure uploading. The two Raman peaks of the E_g mode shift towards high frequency with pressure uploading until 18.9 GPa. However, E_g mode is invisible above 18.9 GPa, which is covered by the intense first-order Raman peak of diamond. Up to 40 GPa, no new Raman peaks appears, indicating the original structure is stable. As shown in Fig. 5(b), the pressure dependence of each vibration mode is linearly fitted, which means each vibration mode has smooth monotonic pressure dependence. The T_{2g}, E_g, and A_{1g} vibration modes depending on the structure are shown in Figs. 4(b)–4(d). As shown in Fig. 5, Raman peaks of

T_{2g}, A_{1g}, and E_g modes exist stable up to 40 GPa and shift to high frequency with pressure as normal. This indicates that the structure of CaB_6 remains stable up to 40 GPa. This is in good agreement with the XRD results. The fitted results are listed in Table 2. Furthermore, the pressure dependence of vibration mode can be represented as the mode-Grüneisen parameter $\gamma_{\omega_i} = -(\partial \ln \omega_i / \partial \ln V) = -(B_0/\omega_i)(\partial \omega_i / \partial P)$, where ω_i represents the phonon frequency, B represents the bulk modulus at ambient conditions, V represents the molar volume, and P represents the pressure. As shown in Table 2, the Grüneisen parameter of E_g mode is the largest one. The Grüneisen parameter describes the vibration mode dependence on the volume of a crystal lattice.

Table 2. Assignment, frequencies, pressure coefficients, and mode-Grüneisen parameters of the Raman vibrational modes of CaB_6.

Vibration mode	ω_i/cm^{-1}	$\partial\omega_i/\partial P$/(cm^{-1}/GPa)	γ_i
T_{2g}	777	3.5	0.9
E_g	1137	8.5	1.5
	1147	9.7	1.7
A_{1g}	1279	9.1	1.4

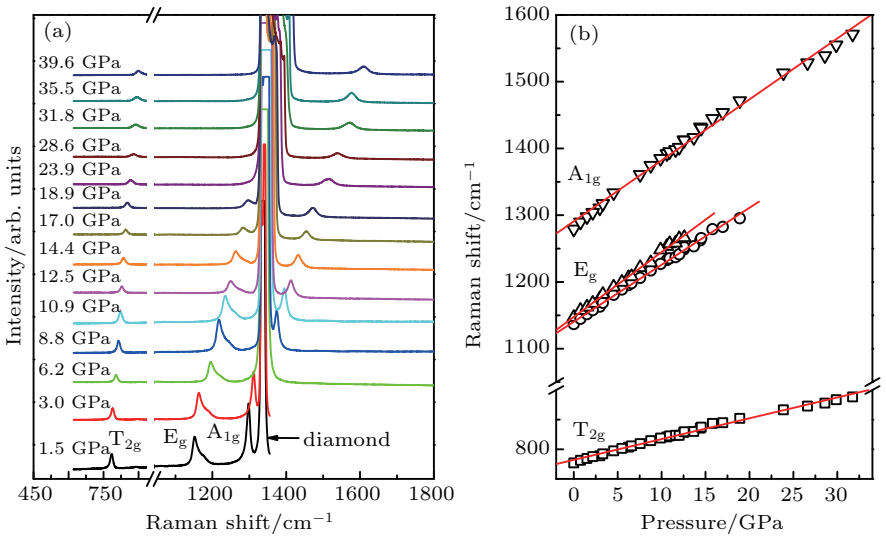


Fig. 5. (a) Selected Raman spectra of CaB_6 measured with pressure uploading, and (b) Raman shift with pressure for main vibrational of CaB_6; the open symbols represent the results of the first run compression while filled symbols represent the second run compression. The lineally fitted data is marked by dotted lines.

The Raman frequency shift of the vibration modes with pressure is related to the change of bond length or bond angle. We have calculated the bond length in boron octahedron and bond length of the neighbouring boron octahedron under high pressure with the Material Studio program. Figure 6 shows B–B_{inter} bond and B–B_{intra} bond length change with pressure. The data is linearly fitted: $k_{intra} = -0.00231$ Å/GPa, $k_{inter} = -0.00309$ Å/GPa. For CaB_6, six boron atoms form an octahedron connected by covalent bonds in the simple cubic crystal structure. Furthermore, covalent bonds connect the octahedron with other six closest octahedrons, and they form a three-dimensional network together. Due to this strong covalent network, the framework of the *Pm*-3*m* structure is very stable. This also explains that the ambient cage structure (*Pm*-3*m*) with a basic covalent network remains stable during the whole experimental pressure run. The bond length in boron octahedron and bond length of the neighbouring boron octahedron change linearly and steadily with pressure, indicating that the structure remains stable and is compressed evenly with pressure. Based on these results, no phase transitions occur in CaB_6 with pressure increasing up to 40 GPa.

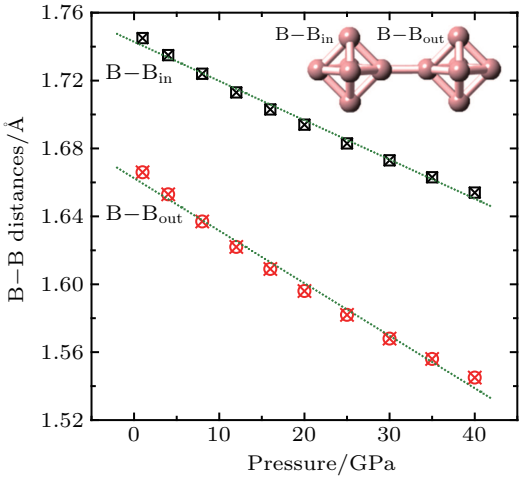


Fig. 6. The B–B distances of CaB_6 at different pressures.

4. Conclusions

In this work, we have successfully studied the structural stability and vibrational characteristics of CaB_6 by means of *in situ* high pressure Raman spectra and synchrotron x-ray diffraction. As pressure increases up to 40 GPa, no phase transitions occur and the lattice constant decreases linearly with pressure. Upon compression, all the vibration modes have

smooth monotonic pressure dependence. The Grüneisen parameter of E_g modes is the largest, indicating its largest dependence on the volume of a crystal lattice. Our experimental results reveal that the covalent network of CaB_6 is difficult to break only under pressure conditions. To promote the occurrence of phase transition, it must be supplied with an alternative pathway to break the energy barrier and further studies are required.

References

[1] Loboda P I, Kysla H P, Dub S M and Karasevs'ka O P 2009 *Mater. Sci.* **45** 108
[2] Takeda M , Terui M, Takahashi N and Ueda N 2006 *J. Solid State Chem.* **179** 2823
[3] Kimura S, Nanba T, Tomikawa M, Kunii S and Kasuya T 1992 *Phys. Rev. B* **46** 12196
[4] Lee B and Wang L W 2005 *Appl. Phys. Lett.* **87** 262509
[5] Joss W, van Ruitenbeek J M, Crabtree G W, Tholence J L, van Deursen A P J and Fisk Z 1987 *Phys. Rev. Lett.* **59** 1609
[6] Ji X H, Zhang Q Y, Xu J Q and Zhao Y M 2011 *Prog. Solid State Chem.* **39** 51
[7] Xu Y, Zhang L J, Cui T, Li Y, Xie Y, Yu W, Ma Y M and Zou G T 2007 *Phys. Rev. B* **76** 214103
[8] Tarascon J M, Etourneau J, Dordor P, Hagenmuller P, Kasaya M and Coey J M D 1980 *J. Appl. Phys.* **51** 574
[9] Popov I, Baadji N and Sanvito S 2012 *Phys. Rev. Lett.* **108** 107205
[10] Young D P, Hall D, Torelli M E, Fisk Z, Sarrao J L, Thompson J D, Ott H R, Oseroff S B, Goodrich R G and Zysler R 1999 *Nature* **397** 412
[11] Vonlanthen P, Felder E, Degiorgi L, Ott H R, Young D P, Bianchi A D and Fisk Z 2000 *Phys. Rev. B* **62** 10076
[12] Tromp H J, van Gelderen P, Kelly P J, Brocks G and Bobbert P A 2001 *Phys. Rev. Lett.* **87** 016401
[13] Zhitomirsky M E, Rice T M and Anisimov V I 1999 *Nature* **402** 251
[14] Zhitomirsky M E and Rice T M 2000 *Phys. Rev. B* **62** 1492
[15] Cao J X, Zhu Y, Yang Z Q and Wu R Q 2009 *Phys. Rev. B* **79** 132404
[16] Song M, Yang I S, Kim J Y and Cho B K 2006 *Vib. Spectrosc.* **42** 288
[17] Godwal B K, Petruska E A, Speziale S, Yan J, Clark S M, Kruger M B and Jeanloz1 R 2009 *Phys. Rev. B* **80** 172104
[18] Cooley J C, Aronson M C, Sarrao J L and Fisk Z 1997 *Phys. Rev. B* **56** 14541
[19] Li M, Yang W, Li L, Wang H, Liang S and Gao C 2011 *Physica B* **406** 59
[20] Kolmogorov A N, Shah S, Margine E R, Kleppe A K and Jephcoat A P 2012 *Phys. Rev. Lett.* **109** 075501
[21] Shah S and Kolmogorov A N 2013 *Phys. Rev. B* **88** 014107
[22] Klotz S, Chervin J C, Munsch P, Le March and G 2009 *J. Phys. D: Appl. Phys.* **42** 075413
[23] Mao H K, Bell P M, Shaner J W and Steinberg D J 1978 *J. Appl. Phys.* **49** 3276
[24] Hammersley A, Svensson S, Hanfl, M, Fitch A and Hausermann D 1996 *High Press. Res.* **14** 235
[25] Young R A 1993 *The Rietveld Method, IUCr Monographs on Crystallography* (Oxford: Oxford Science Publication)
[26] Jr. H and Lin M S 1968 *Solid State Commun.* **6** 379
[27] Wei Y K, Yu J X, Li Z G, Cheng Y and Ji G F 2011 *Physica B* **406** 4476
[28] Birch F 1938 *J. Appl. Phys.* **9** 279
[29] Otani S 1998 *J. Cryst. Growth* **192** 346
[30] Goncharov A F 2012 *Int. J. Spectro.* **2012** 617528
[31] Tang R L, Li Y, Tao Q, Li N N, Li H, Han D D, Zhu P W and Wang X 2013 *Chin. Phys. B* **22** 066202
[32] Lacina D and Gupta Y M 2014 *J. Chem. Phys.* **141** 084503
[33] Ogita N, Nagai S, Okamoto N, Ig F, Kunii S, Akamtsu T, Akimitsu J and Udagawaa M 2004 *J. Solid State Chem.* **177** 461